Transition pathway in GaAs under uniaxial stress: an *ab initio* study

2006 J. Phys.: Condens. Matter 18 4887

(http://iopscience.iop.org/0953-8984/18/20/013)

INSTITUTE OF PHYSICS PUBLISHING JOURNAL OF PHYSICS: CONDENSED MATTER

J. Phys.: Condens. Matter **18** (2006) 4887–4894 doi:10.1088/0953-8984/18/20/013

Transition pathway in GaAs under uniaxial stress: an *ab initio* study

Murat Durandurdu

Department of Physics, University of Texas at El Paso, El Paso, TX 79968, USA

Received 28 March 2006, in final form 17 April 2006
Published 2 May 2006
Online at stacks.iop.org/JPhysCM/18/4887

Abstract

We study the behaviour of GaAs under a uniaxial compression using an *ab initio* constant-pressure technique and find that GaAs undergoes a first-order phase transition to a side-disordered orthorhombic $Imm2$ structure via an intermediate state having the space group of $I\bar{4}m2$. The transition pathway and mechanism under uniaxial stress are found to be considerably different from those under the hydrostatic compression.

1. Introduction

There have been considerable research efforts to understand the behaviour of materials under high stresses. Most studies have focused on simple loading conditions such as hydrostatic pressure or uniaxial tension and have significantly improved our understanding of solid-to-solid phase transitions and the mechanical properties of materials. Nevertheless, remarkable behaviours might be governed by changing the degree of hydrostatic pressure or applying uniaxial compressions. These conditions, however, cannot be easily controlled in experiments and thus reliable simulations play a key role in exploring their influences on materials. Here, using a constant-pressure *ab initio* technique, we show that the application of a uniaxial stress produces a different transformation mechanism in GaAs than expected. Specifically, the zinc blende (ZB) structure does not transform into a $Cmcm$ structure, but instead undergoes a first-order phase transition into an orthorhombic state with space group $Imm2$. The transition occurs via a fourfold coordinated intermediate structure having the space group of $I\bar{4}m2$. These findings can be helpful in understanding the basic physics underlying high-pressure phenomena and the mechanical properties of GaAs and other ZB-type crystalline materials.

GaAs has outstanding physical properties and is of technological importance for electronic and optoelectronic applications. A number of experimental and theoretical studies have been carried out to better understand its pressure-induced phase transitions [1–7]. An earlier x-ray diffraction study [1] synthesized several high pressure phases of GaAs at room temperature: GaAs-I (ZB) → GaAs-II → GaAs-III ($Imm2$) → GaAs-IV (simple hexagonal) at about 17, 24 and 60–80 GPa respectively. This study assigned GaAs-II as an orthorhombic structure with $Pmm2$ symmetry. However, recent experiments using the angle-dispersive technique [4]

revealed that GaAs-II did indeed have $Cmcm$ symmetry. Furthermore, the experiments found no indication of a phase transition to GaAs-III above 24 GPa.

Mujica and Needs [6] performed a first-principles calculation and found that the $Cmcm$ phase was more stable than the $Pmm2$ phase for GaAs. In our preliminary work [7], we studied GaAs under hydrostatic pressures using a constant-pressure *ab initio* technique and found a phase transition from the ZB structure to a $Cmcm$ structure. Moreover, we obtained an $Imm2$ phase with increasing pressure. These results eliminated some doubts about the identity and existence of the high-pressure phases of GaAs.

2. Computational method

The simulation reported here was carried out in a 216-atom model of GaAs which was initially arranged in a ZB structure at an initial lattice parameter $a_\circ = 5.658$ Å. We used a local orbital quantum molecular dynamic method [8]. The essential approximations are (1) nonlocal, norm-conserving pseudopotentials, (2) slightly excited local-orbital basis sets of four orbitals per site, and (3) the Harris functional implementation of density functional theory in the local density approximation. The technique was successfully applied to predict the expanded volume phases of GaAs [9]. Moreover, this Hamiltonian, in conjunction with the Parrinello–Rahman method [10], successfully reproduced the pressure-induced phase transitions in crystalline [7] and amorphous GaAs [11] and in wide range of other amorphous and crystalline materials [12–15], all in agreement with experiments. Only the Γ-point in the Brillouin zone was used, which was reasonable for a 216-atom cell. The atomic coordinates were relaxed until the maximum force was smaller than 0.01 eV Å^{-1}. The structural minimization was performed with a conjugate-gradient technique. Periodic boundary conditions were applied in all directions. A uniaxial stress was employed along the [001] direction, while the other stress components were initially set to zero, and the simulation cell lengths were allowed to adjust to the applied stress.

3. Results

In order to characterize the nature of the phase transition, we first plot the relative volume change as a function of the applied uniaxial stress in figure 1(a). Accordingly, the volume decreases gradually with increasing stress, and at 15 GPa a first-order phase transition occurs with a dramatic volume drop of about 14%. Accompanying this transformation, the simulation cell length compressed declines to a small value while the other two perpendicular dimensions increase to large values, as shown in figure 1(b). The phase at 15 GPa is identified as an orthorhombic state with space group $Imm2$ and is illustrated in figure 2.

In order to understand the transformation mechanism of GaAs under uniaxial compression, we examine the change of the simulation cell lengths and angles as a function of the applied uniaxial stress, and plot their relations in figures 1(b) and (c). The simulation cell vectors $\mathbf{L}_1$, $\mathbf{L}_2$, and $\mathbf{L}_3$ are initially along the [100], [010] and [001] directions, respectively. The magnitude of these vectors is plotted in the figure. As expected, the cell length compressed decreases gradually while the others have a tendency to enlarge because the structure attempts to conserve its volume. The simulation cell angles, on the other hand, remain null until the first-order transition occurs, and hence the simulation box initially changes from cubic to tetragonal. During the transformation at 15 GPa, a triclinic modification of the simulation cell is observed as a result of a small deviation of the simulation cell angles from 90°. Consequently, the cubic $\rightarrow$ tetragonal $\rightarrow$ triclinic adaptation of the simulation cell represents the transformation mechanism of the uniaxially compressed GaAs.

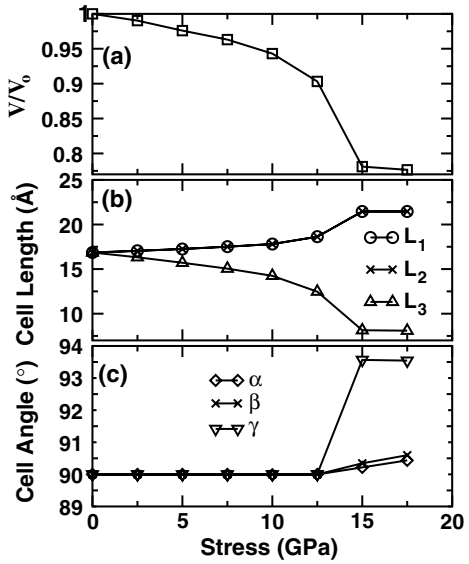

Figure 1. (a) Relative volume change, (b) variation of the simulation cell lengths, and (c) change of the simulation cell angles $\alpha(L_1, L_2)$, $\beta(L_1, L_3)$, and $\gamma(L_2, L_3)$ as a function of the applied uniaxial stress.

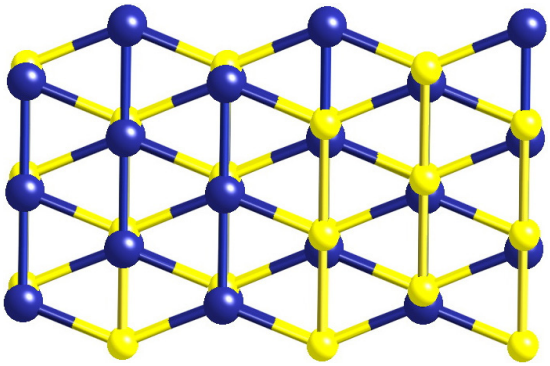

Figure 2. $Imm2$ phase of GaAs produced at 15 GPa with the application of uniaxial stress. For clarity, only a small portion of the simulation cell is shown.
(This figure is in colour only in the electronic version)

We next analyse the symmetry change of the structure at each applied stress using the KPLOT program [16], which provides detailed information about space group, cell parameters and atomic positions for a given structure. For the symmetry analysis, we use 0.1 Å, 4°, and 0.7 Å tolerances for bond lengths, bond angles and interplanar spacing, respectively. Although the tetragonal modification of the simulation cell is observed below 5 GPa, we are not able to characterize clearly the space group of the structure in this stress range. At 5 GPa, on the other hand, we determine a tetragonal phase with the space group $I\bar{4}m2$. The unit cell parameters of the $I\bar{4}m2$ phase are $a = b = 4.0663$ Å and $c = 5.2352$ Å. This tetragonal state is still fourfold coordinated with a bond length of 2.38 Å and bond angles of 105.58° and 117.55°.

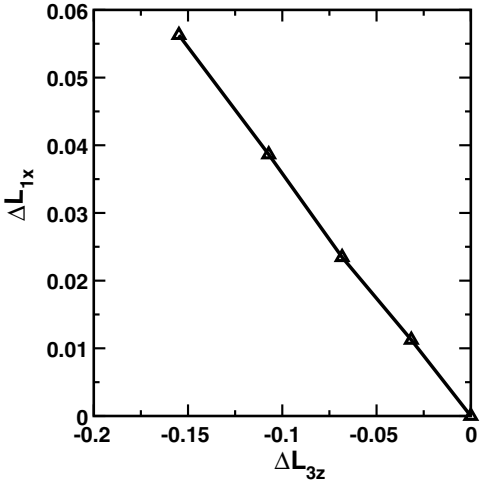

Figure 3. Variation of ΔL_{1x} as a function of ΔL_{3z}.

Table 1. The atomic fractional coordinates and the lattice parameters of the tetragonal $I\bar{4}m2$ phase at 5 GPa and the orthorhombic $Imm2$ phase at 15 GPa.

Phase	a (Å)	b (Å)	c (Å)		x	y	z
Tetragonal $I\bar{4}m2$	4.0663	4.0663	5.2352	Ga:	0.0	0.0	0.0
				As:	0.0	0.5	0.25
Orthorhombic $Imm2$	5.2130	4.8983	2.7133	Ga:	0.0	0.0	0.215 429
				As:	0.0	0.5	0.581 949

The $I\bar{4}m2$ symmetry of the structure is maintained up to 15 GPa, at which point a sixfold coordinated orthorhombic state is formed. The orthorhombic phase has $Imm2$ symmetry and is characterized by the lattice constants $a = 5.2130$, $b = 4.8983$ and $c = 2.7133$ Å. The $Imm2$ crystal has four unlike neighbours at a distance of 2.3 Å and two like neighbours at 2.5 Å, and thus it is a side-disordered structure. The lattice parameters and the atomic positions of both phases are summarized in table 1.

The relations between the simulation cell (216 atoms) and the unit cells are also determined by the KPLOT program. For the ZB structure, the unit cell vectors **a**, **b** and **c** are parallel to the simulation cell vectors $\mathbf{L}_1$, $\mathbf{L}_2$ and $\mathbf{L}_3$, and hence $\mathbf{a} = \mathbf{L}_1/3$, $\mathbf{b} = \mathbf{L}_2/3$ and $\mathbf{c} = \mathbf{L}_3/3$. With the modification to the tetragonal phase, the unit cell vectors become $\mathbf{a} = (\mathbf{L}_1 + \mathbf{L}_2)/6$, $\mathbf{b} = (\mathbf{L}_1 - \mathbf{L}_2)/6$, and $\mathbf{c} = -\mathbf{L}_3/3$. For the orthorhombic state the unit cell vectors can be calculated using the following relations: $\mathbf{a} = (-\mathbf{L}_1 + \mathbf{L}_2)/6$, $\mathbf{b} = -(\mathbf{L}_1 + \mathbf{L}_2)/6$, and $\mathbf{c} = \mathbf{L}_3/3$.

From the stress–simulation cell lengths relation, we can calculate the Poisson ratio that is used to characterize a material's elastic properties. The Poisson ratio of a solid subjected to a uniaxial stress is defined as the negative ratio of transfer strain in the i direction resulting from an applied strain in the j direction. The Poisson ratio for a cubic simulation box compressed uniaxially along the L_{3z} direction is determined by

$$\sigma_{13} = -\frac{\Delta L_{1x}}{\Delta L_{3z}}. \tag{1}$$

The variation of ΔL_{3z} and ΔL_{1x} in the pressure range 0–10 GPa is given in figure 3. The slope

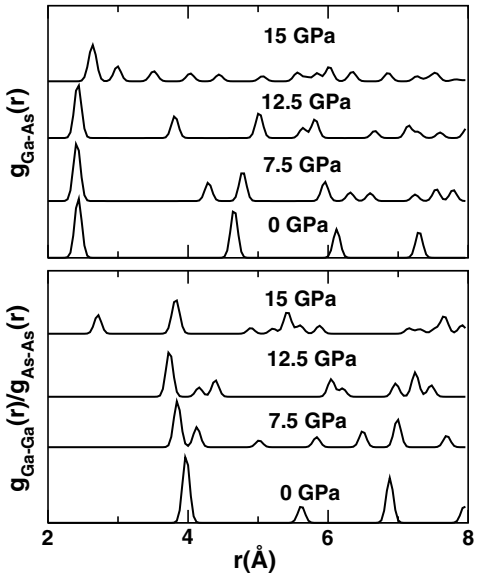

Figure 4. Partial pair distribution functions as a function of uniaxial stress.

of the best fitting straight line gives 0.36 for the Poisson ratio of GaAs at zero pressure. This value is less than the experimental result of 0.44 [18].

In order to analyse the structural changes through the transition, we plot the partial pair distribution functions (PDFs) in figure 4. There is relatively no change seen in the first neighbour Ga–As distance up to 15 GPa, implying that the bond lengths are almost invariant under uniaxial compression. This differs from the hydrostatic case in which the first neighbour distance decreases gradually with increasing pressure. At 15 GPa, the first neighbour Ga–As peak moves abruptly to a higher distance with a broadened distribution and reduced intensity, which reflects a clear indication of a phase transition into a higher coordinated structure. On the other hand, the second and third neighbour distances decrease monotonically due to the angular distortions (see below) and hence the transition results from a significant decrease of the second neighbour distances. It should be noted that the Ga–Ga and As–As distances gradually decrease with increasing uniaxial stress, and as for the phase transition, these separations abruptly decrease to a small value. This indicates the formation of the Ga–Ga and As–As homopolar bonds and hence a side-disordered $Imm2$ phase.

The microscopic structural changes are further analysed in terms of the bond angle distribution function given in figure 5. Accordingly, the structure undergoes dramatic angular distortions because of the simultaneous compression and expansion of the system with the application of uniaxial stress. The tetragonal angles gradually tend towards 146° and 94°, at which points the $Imm2$ structure is formed. By opening tetragonal angles, the second nearest neighbour distances are decreased, bringing the second neighbour atoms closer to form a sixfold coordinated structure. The opening of the tetragonal angles without changing the bond lengths does indeed indicate that the transition under uniaxial stress results from bond bending and hence is different from the hydrostatic conditions.

4. Discussion

These observations indicate that the transition paths followed under uniaxial compression (ZB $\rightarrow$ $I\bar{4}m2$ $\rightarrow$ $Imm2$) differ from the ZB $\rightarrow$ $Cmcm$ $\rightarrow$ $Imm2$ transitions under

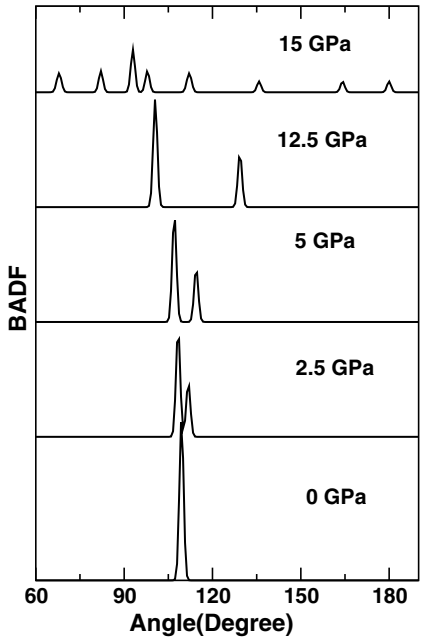

Figure 5. Bond angle distribution function under uniaxial compression.

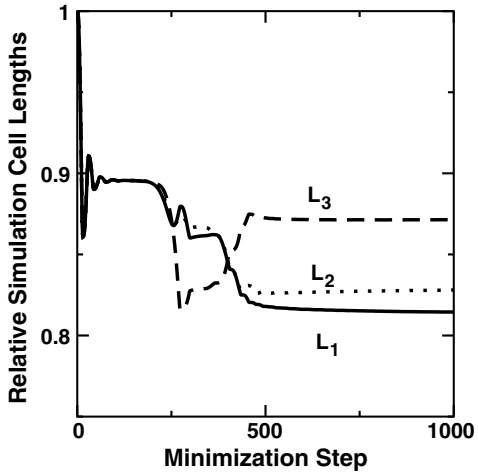

Figure 6. Change of the simulation cell lengths during the formation of the $Cmcm$ phase as a function of minimization step at 54 GPa under hydrostatic pressure.

hydrostatic pressure. This distinct behaviour can be understood by examining how the ZB structure responds differently to both loading conditions. Under uniaxial stress, the simultaneous compression and expansion lead to the symmetry breaking and the formation of both $I\bar{4}m2$ and $Imm2$ phases. Such a mechanism, however, does not exist in the case of hydrostatic pressure in which the structure is isotropically compressed along all directions and the symmetry is preserved until a phase transition occurs. Furthermore, as is shown in figure 6, during the formation of the $Cmcm$ phase, a dramatic compression along all directions is seen:

at least two axes must be more compressed than the other. Consequently the transformation mechanism seen in the uniaxial and hydrostatic conditions differs significantly from each other and leads to different structures.

Another interesting observation is a significant reduction of the transition pressure of the $Imm2$ phase under uniaxial stress (15 GPa), relative to the hydrostatic pressure value of 57 GPa in the simulation. This observation agrees with recent thermodynamic analysis [17]. The physical origin of such a lower transition pressure is associated with bond bending.

In the previous study, we have shown that both hydrostatically and uniaxially compressed germanium (Ge) transform to a β-Sn phase. However, the transformation mechanisms are found to be different for two loading conditions. In the uniaxial case, the transition involves bond bending and the transition pressure is significantly reduced, similarly to what we have determined for GaAs. General tendencies seen in Ge and GaAs under uniaxial stress show striking similarities even though they transform into different structures. Therefore, we expect to see analogous transformation mechanisms and probably the formation of β-Sn, $Imm2$ or closely related structures in other diamond and ZB structured materials. It should be noted that both uniaxially compressed Ge and GaAs transform to a phase that has also been formed under hydrostatic pressure; however, not all ZB structured systems subjected to hydrostatic pressure convert into a β-Sn phase or an $Imm2$ phase. Consequently, uniaxial compressions might yield a new phase in these systems. It would, therefore, be interesting to study the response of other ZB structured materials to uniaxial compressions.

5. Conclusion

The response of GaAs to a uniaxial stress has been studied using an *ab initio* constant-pressure simulation. The ZB structure transforms into a tetragonal state with space group $I\bar{4}m2$. This phase is still fourfold coordinated with a large angle deviation from the ideal tetrahedral angle. Upon further increase of the applied uniaxial stress, the tetragonal structure undergoes a first-order phase transition into a sixfold coordinated $Imm2$ structure at 15 GPa. This observation is particularly important because it suggests that we might control transition mechanisms by changing the degree of loading conditions. Furthermore, we argue that the formation of β-Sn, $Imm2$ or closely related structures is likely to occur in the diamond and ZB structured materials under uniaxial compressions.

Acknowledgments

The author is grateful to Professor D A Drabold for providing the FIREBALL96 MD code and Professor E Hagedorn for reading the paper.

References

[1] Weir S T, Vohra Y K, Vanderborg C A and Ruoff A L 1989 *Phys. Rev.* B **39** 1280
[2] Zhang S B and Cohen M L 1989 *Phys. Rev.* B **39** 1450
[3] Besson J M, Itié J P, Polian A, Weill G, Mansot J L and Gonzalez J 1991 *Phys. Rev.* B **44** 4214
[4] McMahon M I and Nelmes R J 1996 *Phys. Status Solidi* b **198** 389
[5] McMahon M I and Nelmes R J 1997 *Phys. Rev. Lett.* **78** 3697
[6] Mujica A and Needs R J 1996 *J. Phys.: Condens. Matter* **8** L237
[7] Durandurdu M and Drabold D A 2002 *Phys. Rev.* B **66** 045209
[8] Sankey O F and Niklewski D J 1989 *Phys. Rev.* B **40** 3979
[9] Demkov A A, Sankey O F, Gryko J and McMillan P F 1997 *Phys. Rev.* B **55** 6904
[10] Parrinello M and Rahman A 1980 *Phys. Rev. Lett.* **45** 1196

[11] Durandurdu M 2004 *Phys. Rev.* B **70** 085204
[12] Durandurdu M 2005 *Phys. Rev.* B **71** 054112
[13] Durandurdu M and Drabold D A 2001 *Phys. Rev.* B **64** 014101
[14] Durandurdu M and Drabold D A 2002 *Phys. Rev.* B **66** 041201
[15] Durandurdu M and Drabold D A 2002 *Phys. Rev.* B **65** 104208
[16] Hundt R, Schön J C, Hannemann A and Jansen M 1999 *J. Appl. Phys.* **32** 413
[17] Cheng C, Huang W H and Li H J 2001 *Phys. Rev.* B **63** 153202
[18] Hellwage K H (ed) 1982 *Numerical Data and Functional Relations in Science and Technology* vol 17a *Physics of III–V Compounds* (Berlin/Heidelberg/New York: Madellung/Springer)